ARCHIVES OF TRANSPORT
Volume 68, Issue 4, 2023

ISSN (print): *0866-9546*
e-ISSN (online): *2300-8830*
DOI: *10.61089/aot2023.k0c5b837*

THE APPLICATION OF TIME-FREQUENCY METHODS OF ACOUSTIC SIGNAL PROCESSING IN THE DIAGNOSTICS OF TRAM DRIVE COMPONENTS

Daniel MOKRZAN[1], Tomasz NOWAKOWSKI[2], Grzegorz M. SZYMAŃSKI[3]

[1, 2, 3] Poznan University of Technology, Institute of Transport, Poznań, Poland

Abstract:

The paper presents the course of investigations and the analysis of the possibility of applying selected methods of time-frequency processing of non-stationary acoustic signals in the assessment of the technical condition of tram drive components, as well as a new combined method proposed by the authors. An experiment was performed in the form of a pass-by test of the acoustic pressure generated by a Solaris Tramino S105p tram. A comparative analysis has been carried out for an efficient case and a case with damage to the traction gear of the third bogie in the form of broken gear teeth. The recorded signal was analyzed using short-time Fourier transform (STFT) and continuous wavelet transform (CWT). It was found that the gear failure causes an increase in the sound level generated by a given bogie for frequencies within the range of characteristic frequencies of the tested device. Due to the limitations associated with the fixed window resolution in STFT and the inability to directly translate scales to frequencies in CWT, it was found that these methods can be helpful in determining suspected damage, but are too imprecise and prone to errors when the parameters of both transforms are poorly chosen. A new CWT-Cepstrum method was proposed as a solution, using the wavelet transform as a pre-filter before cepstrum signal processing. With a sampling rate of 8192 Hz, a db6 mother wavelet, and a scale range of 1:200, the new method was found to infer the occurrence of damage in an interpretation-free manner. The results were validated on an independent pair of trams of the same model with identical damage and as a reference on a pair of undamaged trams demonstrating that the method can be successfully replicated for different vehicles.

Keywords: *acoustic pressure, time-frequency methods, tram drive diagnostics, cepstrum, shorttime fourier transform, continuous wavelet transform*

To cite this article:

Mokrzan, D., Nowakowski, T., Szymański, G.M., (2023). The application of time-frequency methods of acoustic signal processing in the diagnostics of tram drive components. Archives of Transport, 68(4), 55-75. DOI: https://doi.org10.61089/aot2023.k0c5b837

Contact:
1) daniel.mokrzan@doctorate.put.poznan.pl [http://orcid.org/0000-0001-8274-7009] – corresponding author;
2) tomasz.nowakowski@put.poznan.pl [http://orcid.org/0000-0001-5415-7052];
3) grzegorz.m.szymanski@put.poznan.pl [http://orcid.org/0000-0002-2784-9149];

1. Introduction

In the operation of machinery one of the most effective and at the same time economical methods of diagnosis is the analysis of technical condition on the basis of vibroacoustic signal processing. This term is understood as time realization of phenomena of wave character, representing mechanical and acoustic vibrations which are accompanying processes (Cempel, 1992). Variability of signals in time within a wide frequency band constitutes a large information resource, sensitive to any changes in the system, including the occurring damages. At the same time the available methods of the vibroacoustic signal acquisition allow to obtain it in a non-destructive way and without disturbing the operation of the device (Randall, 2011). These methods allow for both diagnosis of devices, whose work in the standard cycle of exploitation is characterized by the occurrence of vibration, e.g. rotating machines (Bouaouiche et al., 2023; Chen et al., 2016; Jałowiecki et al., 2021; Shim et al., 2021), but also with the use of appropriate excitation also of elements which do not generate vibrations during normal operation, e.g. composite housing elements (Katunin et al., 2015; Mokrzan et al., 2021), beams or turbine blades (Milewicz et al., 2021).

Most of the physical systems occurring in reality are characterized by non-linearity, which meet the assumptions of linearity only in the case of vibrations with low amplitudes. As a result, most of the signals recorded and processed during the operation of machines and vehicles are non-stationary. This non-stationarity does not have to result from the assumed initial non-linearity of the system. It can change over time, as exemplified by the effect of emerging defects in the technical equipment on the recorded signal. Each stage of use of a technical device is affected by defects that impact the signals of processes occurring during the operation of the machine, ranging from imperfections during design and manufacture to failures caused by overuse. In addition, the very nature of the technical object's operation may be non-stationary, e.g., variable speed during use or variable speed of movement (Randall, 2011).

The problem of non-stationary signal processing is also related to vibroacoustic diagnosis of rail vehicle components (Mokrzan & Szymański, 2021). It results both from the nature of damage and the chosen method of testing and measurement. In the first case, the aim is to identify not only the damage form, but also its location. Traditional stationary methods of signal analysis, including Fourier analysis, are insufficient in this case (Huang et al., 1998; Mandic et al., 2013). An example would be the identification of flat spots in the wheel of a rail vehicle. Using the frequency spectrum of the signal and their combination may be sufficient to determine that such a phenomenon occurs (Nowakowski et al., 2019). However, simultaneous time domain analysis is required to pinpoint the exact location of the damage (Liang et al., 2013). This implies the use of non-stationary signal analysis methods. Analogous difficulties occur in the case of selected methods of vibroacoustic signal acquisition.

Among non-stationary signal analysis methods, time-frequency methods are characterized by high efficiency. They allow simultaneous decomposition of the signal in time and frequency, which makes it possible to determine the nature of damage and its localization at the same time (Mokrzan & Szymański, 2021).

One of the most important issues in the development of sustainable transport is the early detections of occurrence of damages which may affect the environment (Milewicz et al., 2023). This paper will analyze the possibility of using two time-frequency analysis methods - short-time Fourier transform (STFT) and continuous wavelet transform (CWT) in identification of occurrence and location of damage of drive system of selected rail vehicle in pass-by test. In addition, as a proposed solution to the limitations of these methods, a proposal for a new combined method will be presented, using both the method of analyzing non-stationary signals - wavelet transform, as well as the method of analyzing stationary signals - cepstrum.

2. Vibroacoustic signal processing

2.1. Signal stationarity criterion

To determine the stationarity of the process it is necessary to know the mean value described by equation (1) and the correlation function expressed by the relation (2).

$$m_s(t_1) = \lim_{N\to\infty} \frac{1}{N} \sum_{k=0}^{N-1} s_k(t_1), \tag{1}$$

$$R_s(t_1, t_1+\tau) = \lim_{N\to\infty} \frac{1}{N} \sum_{k=0}^{N-1} s_k(t_1) \cdot s_k\,(t_1+\tau) \tag{2}$$

The stochastic process $\{s(t)\}$ can be non-stationary or stationary in a broader sense (weakly stationary) and in a narrower sense (strictly stationary). It is defined as non-stationary if its mean values and autocorrelation function are time dependent. A process is stationary in a broader sense (weakly stationary) when the values of the function $m_s(t_1)$ i $R_s(t_1, t_1+\tau)$ do not depend on time t. In practice, this means that the mean value of weakly stationary processes is constant, and the autocorrelation function depends only on the shift τ, i.e. $m_s(t_1) = m_s$ and $R_s(t_1,t_1+\tau) = R_s(\tau)$.

If for the stochastic process $\{s(t)\}$ an infinite set of higher order and combined moments can be calculated and if all possible moments and combined moments do not depend on process time, then the process $\{s(t)\}$ is called strictly stationary or stationary in a narrower sense.

If statistical functions are used to describe the stochastic process, i.e., the mean value written in the form of relation (3) and the autocorrelation function (4), then if the random process $\{s(t)\}$ is stationary and the values $m_s(k)$ and $R_s(\tau,k)$ determined by formulas (3) and (4) are the same for different random functions, then such a random process is called ergodic. If the signal is ergodic then on the basis of analysis of one realization one can infer the whole population of realizations.

$$m_s(k) = \lim_{N\to\infty} \frac{1}{T}\int_0^T s_k(t)dt, \tag{3}$$

$$R_s(\tau,k) = \lim_{N\to\infty} \frac{1}{T}\int_0^T s_k(t)\cdot s_k(t+\tau)dt, \tag{4}$$

The analysis of relations (1) to (4) leads to the conclusion that ergodic processes are a special case of stationary processes (Park, 2018).

2.2. Cepstrum

Cepstrum is one of the methods of stationary frequency analysis. It is one of the older methods of signal processing, having been developed two years before the first FFT algorithm was created (Bogert et al., 1963). Cepstrum was defined in 1963 by Bogert, Healy and Tukey. The word is an anagram of the word spectrum to justify its origin from traditional Fourier analysis. Three forms of cepstrum are used in signal analysis: complex (Eq. 5), power (Eq. 6) and real (Eq. 7).

$$C_c(\tau) = F^{-1}\{\ln(A(f) + i\varphi(f)\} \tag{5}$$

$$C_p(\tau) = F^{-1}\{2ln(A(f))\} \tag{6}$$

$$C_r(\tau) = F^{-1}\{ln(A(f))\} \tag{7}$$

where A(f) is the amplitude spectrum of the signal, iφ(f) is the phase spectrum of the signal, and F^{-1} is the inverse form of the Fourier transform (Randall, 2017).

From the equations presented, it follows that the composite form of the cepstrum contains information about the phase of the signal. Thus it allows to fully reproduce it. The real and power forms of the cepstrum are devoid of this dependence. Analyzing equations (6) and (7) it can be deduced that one is a scaled version of the other.

The cepstrum method consists in subjecting the analyzed signal to the Fourier transformation, thanks to which a frequency representation is obtained, which is then transformed to a logarithmic scale. This result is then subjected to Inverse Discrete Fourier Transform (IDFT) in case of sampled signals. Successive values on the ordinate axis of the waveform can be interpreted as units of time, while values on the cut-off axis are related in some way to the autocorrelation and the fundamental tone can be determined from them. Cepstrum can be defined as information about the rate of change in the frequency bands of the frequency spectrum of the analyzed signal (Randall, 2017).

Despite its age, Cepstrum is one of the less known and less used signal processing methods in terms of machine diagnostics. Randall believes, however, that the capabilities of the method have not yet been fully exploited and it is potentially amenable to further development (Randall, 2017).

2.3. Time-frequency methods

One approach to analyzing non-stationary signals is to use methods that use joint time-frequency (t/f) representations of the signals (Joint Time-Frequency Analysis, JTFA) (Mokrzan & Szymański, 2021). A graphic example of such a combined representation compared to time and frequency domain representations is shown in Fig. 1.

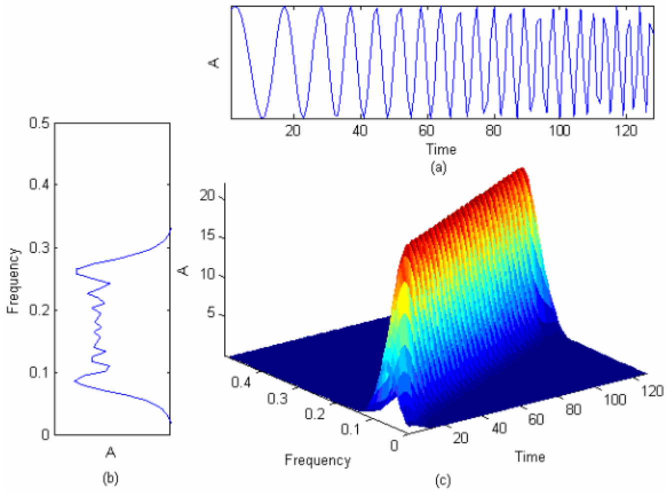

Fig. 1. Comparison of signal representation in time, frequency and time-frequency domains (Zhu et al., 2012)

The summary of characteristics shown in Fig. 1 visualizes the differences between the time, frequency, and time-frequency representations of the signal. The diagnostic usefulness of the latter is also clearly visible. Analyzing only the overall spectrum of the signal it is difficult to obtain feedback suitable for making diagnostic inferences - it is difficult to distinguish possible dominant components. Using JTFA such information is obtained - signal is non-stationary, characterized by single dominant frequency component, which undergoes phase shift with time. Such unambiguously formulated signal description allows to use it for precise diagnostic inference.

2.3.1. Short-time Fourier transform

Short-time Fourier transform can be defined as subjecting to spectral analysis, using FFT, short signal sequences treated as quasi-stationary. The division of the input signal into successive analyzed segments is realized using a technique called moving window. Representation of the spectra obtained in this way on a single characteristic allows to obtain time-frequency representation of the analyzed process called spectrogram. STFT can be defined by the following equation 8 (Szymański et al., 2017).

$$STFT[x_w(t,\tau)] = \int_{-\infty}^{\infty} w(t,\tau)x(t) \cdot e^{-i2\pi ft}dt \quad (8)$$

where: $x(t)$ – representation of the analyzed input signal in time domain, τ – position of the moving window in the time domain, $x_w(t,\tau) = w(t-\tau)x(t)$ – extracted analyzed data segment.

Thus, the STFT result can be interpreted as a sequence of spectra determined for shorter, local time fragments. The advantages of this method include short computation time required to determine the spectrogram, the requirement of negligible computational power and constant resolution over the entire spectral range. Moreover, the use of STFT for signal interpretation can be assessed as easy and intuitive compared to other methods. The major disadvantages of this method include the inability to simultaneously obtain high window resolution for time and frequency (Heisenberg indeterminacy principle). It is possible to minimize the negative effects of this limitation by using the *overlapping* method, which consists in partial overlapping of the analyzed signal segments. As a result, increased resolution in time domain is obtained without the necessity of its decrease in frequency domain (Szymański et al., 2017).

2.3.2. Wavelet transform

In order to effectively analyze the spectral properties of non-stationary signals, there is a need to look at them over a sufficiently wide and traversable interval. This requirement can be formulated as the need

to use windows that automatically narrow when analyzing high frequencies and analogously expand when analyzing low frequencies. These properties are possessed by wavelet-based integral transforms through the use of scaling (Batko & Ziółko, 2002). In the wavelet transform, the wavelets are called mother functions. These can be any functions. Application of this wavelet enables use of FFT procedure in processing, as a result accelerating computation process. The form of the result depends on adopted mother functions, that is why the essential process of signal analysis is adequate selection of wavelet (Komorski et al., 2018).
There are two forms of wavelet transform - continuous and Discrete Wavelet Transform (DWT). CWT can be defined by equation 9 (Newland, 1997).

$$CWT_{\Psi}(a,b) = \frac{1}{\sqrt{a}} \int_{-\infty}^{+\infty} x(t) \cdot \Psi^{*}\left(\frac{t-b}{a}\right) dt \qquad (9)$$

where: $\Psi(t\text{-}\tau)$ – mother function, $x(t)$ – continuous signal in the time domain, a – scale parameter, b – shift parameter (place), Ψ^{*} – coupling of functions $\Psi(t\text{-}\tau)$
The continuous wavelet transform can be represented as the sum over all time of a signal multiplied by a scaled, shifted version of the wavelet. The result of this process is the determination of so-called wavelet coefficients, which are a function of scale and shift. The described type of analysis can be compared to filtering with constant relative bandwidth $\Delta f/fs$. The position of the filter on the time-scale representation is determined by the scale and shift parameters (a, b). As one moves toward higher frequencies, the bandwidth of the analysis increases while the resolution of the analysis in the frequency domain decreases, while the resolution in the time domain increases in turn. This feature is potentially useful for simultaneous analysis and observation with different time step of processes characterized by fast variability and large amplitudes of frequency components, e.g. valve operation, combustion process and similarly slow-variable low-frequency processes. The difference between the scaled windows characteristic for the WV transformation and the windows with constant resolution characteristic for the STFT transformation are shown in Fig. 2. The disadvantages of the described method include dependence of the result form on the assumed basis function and not always intuitive interpretation of the graphic result. (Rhif et al., 2019).
Computing wavelet coefficients for every possible scale (the scale domain is continuous) requires a large amount of work and computational time while generating a large volume of data.
The solution is to limit the subset of scales and positions for which calculations will be performed (scale domain is discrete). In order to increase the accuracy of the calculations, scales and positions based on the power of two are used, so called dyadic. For this purpose four wavelet filters are applied: high pass and low pass and their equivalents for the Inverted Discrete Wavelet Transform (IDWT). The result of the described actions is the separation of the signal into two wavelet coefficients, the first cA with a large scale value describing the approximation component A, and the second cD with a smaller scale value representing the detail component D. IDWT filters are used to reconstruct the original signal based on cA and cD (Jaworek et al., 2001). A block diagram of the execution of the DWT and IDWT process is shown in Figure 3.

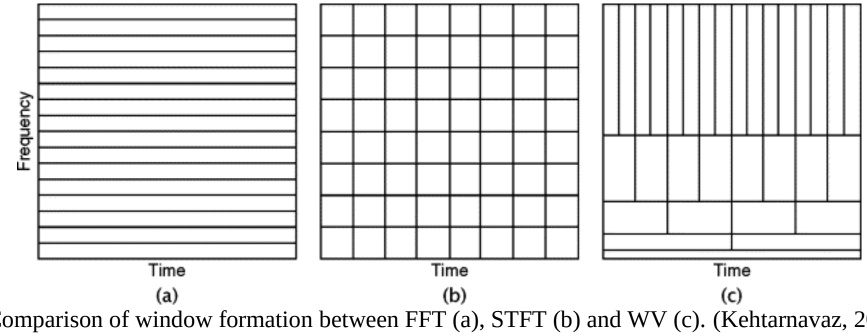

Fig. 2. Comparison of window formation between FFT (a), STFT (b) and WV (c). (Kehtarnavaz, 2008)

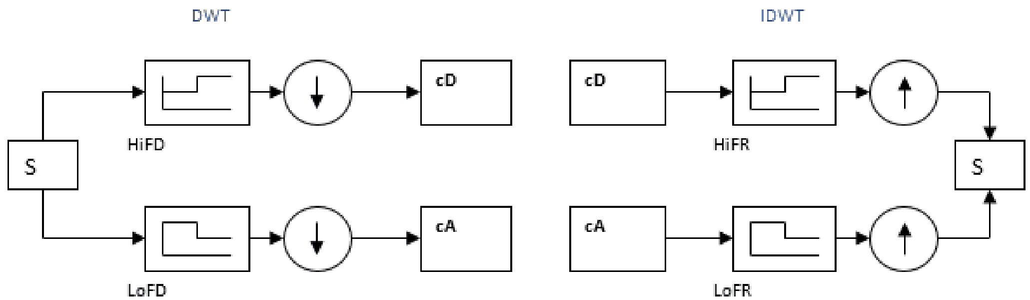

Fig. 3. Discrete wavelet transform of DWT and inverse wavelet transform of IDWT. HiFD - DWT high-pass filter, LoFD - DWT low-pass filter, HiFR - IDWT high-pass filter, LoFR - IDWT low-pass filter. (Jaworek et al., 2001)

Comparing DWT and CWT, it can be concluded that the discrete form of the wavelet transform is useful for decomposition and selective reconstruction of the studied signal in the whole range of analysis. The continuous form of this transform is evaluated as particularly predestined for the study of internal processes of the machine, the manifestation of which is the local variation of the informational variation of external vibroacoustic phenomena, not only limited to the time domain (Batko & Ziółko, 2002).

3. Related work - use of cepstrum and JTFA methods in vibroacoustic diagnostics of machinery and vehicles

Despite its age, cepstrum has never achieved such a wide application in machine diagnostics as the FFT algorithm developed later. Experiences with its use so far, however, give reasons to believe that this method is effective and susceptible to further development. This is indicated, among other things, by the fact that the cepstrum is the subject of continuous research and the resulting publications (Randall, 2017). One of the earliest described applications of the cepstrum is presented in (Randall, 1975). It was used to identify the spacing between the sidebands (and thus between the carrier frequencies) of a vibration signal spectrum from a gearbox, in order to possibly identify anomalies in the overlapping. In (Sapy, 1975), cepstrum was shown to be more effective than spectrum in determining the absence of blades in a steam turbine. The possibility of using cepstral analysis in the interpretation of an acoustic signal was demonstrated, the pressure in each cylinder was determined from the sound generated by a diesel engine (Lyon & Ordubadi, 1982). In a later study, an attempt was made to solve the problem of limiting the cepstrum to stationary signals. A stepwise analysis was performed, the vibration signal in time was divided into smaller sections, each of which was processed separately using the cepstrum, which made it possible not only to find damage in the gearbox but also to localize it (Badaoui et al., 2001). There are also recent publications indicating that cepstrum is developing, e.g. an algorithm to improve rolling bearing damage detection (J. Guo et al., 2021), as well as detecting wear positions of the rotor and stator in the turbine (Yu et al., 2022). In rail vehicle applications, recent research has demonstrated the effectiveness of cepstrum in detecting flat spots on wheel rolling surfaces (Baasch et al., 2021; Shim et al., 2021). Cepstrum was used to remove the effect of transfer function from gear transmission error in operational modal analysis (Lu et al., 2022). Especially, the geometric profile error and stiffness profile, with high resolution, are successfully separated. An example of using the cepstrum method is also presented in the paper (Kim et al., 2021), where it served as an extension of the empirical wavelet transform in planetary gear diagnostics. For this purpose, the vibration signal was decomposed using empirical wavelet filters designed based on the smoothed spectrum from cepstrum analysis. In the paper (Jiang et al., 2021) cepstrum was used to extract the impact features of rolling bearing defects. This method has also been used in economics to provide evidence that inflation targeting has indeed reduced inflation volatility (Antonakakis et al., 2021). Adaptive time delay estimation method for broadcast audio based on power cepstrum is another example (Tang et al., 2020).

The short-time Fourier transform is used in diagnostics of machines and machine components, especially in non-stationary operating states, e.g. for evaluating the technical condition of the rotating machines and rolling elements (Cocconcelli et al., 2012; Liu et al., 2020; Lopez-Ramirez et al., 2016; Ouamara et al., 2023). STFT is used in rail vehicle diagnostics. (Komorski et al., 2018) presents the idea of wheel-flats detection by acoustic signal processing using JTFA methods. The noise generated by a passing tram with an efficient running system and a tram with wheel-flats at three different running speeds was measured. STFT was then used to perform a time-frequency analysis and from this, spectrograms were generated and frequency bands sensitive to the flat spot contact with the rail were identified.

In (Tatara & Kożuch, 2016) an attempt was made to experimentally analyze vibrations generated during the passage of Pendolino EMU 250 trains. The measuring ground was made up of seven vibration transducers located at different distances from the track. The signal of vibrations caused by passing was analyzed in frequency domain using FFT and time-frequency domain STFT. The authors concluded that the decomposition of the vibration signal in the vicinity of the railroad using STFT enables the analysis of the technical condition of individual passing rolling stock components. Observation of the time-frequency map allows determination of time windows associated with specific vehicle components and makes it possible to detect, for example, damage to a wheelset if it generates vibrations larger than the others.

One of the most popular alternatives to STFT is the wavelet transform, both in continuous and discrete form. Its effectiveness in terms of vibro-acoustic diagnosis has been proven during tests for basic machine components such as bearings (Li et al., 2022; Zhao et al., 2023), transmission elements (Dai et al., 2022; Majeed et al., 2023), rotating machines (Saini et al., 2022) or combustion engines (Wu & Chen, 2006). CWT is considered a more effective tool for the analysis of non-stationary signals. Despite its longer computational time, it enables multi-resolution analysis, thus solving the problem of the fixed resolution of the STFT limiting window (Akansu & Haddad, 2001; T. Guo et al., 2022).

Wheel-rail contact issues are an important topic in the field of driving safety and are one of the key issues considered by many researchers (Jacyna et al., 2014; Ortiz et al., 2018; Staśkiewicz & Firlik, 2018). One such issue is the occurrence of wheel slippage. Reasons for its occurrence may be, among others, the appearance of "wheel-flats" on the wheel, damage to the rail surface or braking (Iwnicki et al., 2019). When slippage occurs, longitudinal vibrations appear in relation to the contact line. This can lead to excessive loads and expose the wheel to polygonization (Johansson & Andersson, 2005).

On the basis of the literature analysis, it was concluded that while the described signal processing methods have been successfully used in a number of cases related to the diagnostics of machine components, their implementation in the assessment of the technical condition of rail vehicle components, especially drive systems, is still in the development stage. In particular, there is a lack of comprehensive methods enabling non-invasive diagnostics during standard vehicle operation.

The research described in this article was aimed at developing an original method of vibroacoustic signal processing that fits within the above described niche. Acoustic pressure analysis in pass-by test was chosen because of its simplified acquisition to vibration signal during standard operation of rail vehicles. Moreover, the justification for the chosen diagnostic parameter is the possibility of later practical use of the method. A single station for sound analysis of the moving vehicle would be easier to use in relation to each time the vibration transducers need to be placed in the vehicle.

4. Methodology and research objective

The study was conducted using the basic assumptions of a passive experiment . The parameters of the recorded acoustic signal were observed without prior knowledge of the technical condition of the object. The investigators also had no possibility to control the object, including the way of its movement and speed.

The measurements were performed in favorable weather conditions, without precipitation. The temperature was between 11 and 13 degrees Celsius, the atmospheric pressure was 1 020 hPa, and the wind speed did not exceed 5 m/s.

Sound pressure measurements were conducted from the track position in a pass-by test. A microphone

matrix consisting of 9 microphones (M1-M9) was used to measure sound pressure. The use of matrix measurements was justified by the fact that the analyses performed in this paper represent a section of a broader study focusing, in addition to the development of new signal processing methods, on the analysis of the location of measurement points. The location of the microphones depended on the geometry of the tram running system (scheme in Fig. 4).
Recording began before the test tram entered the measurement cross-section and ended after it left. The sampling frequency was 65 536 Hz. This allowed the acquisition of the signal in the full range of frequency recorded by the microphone. The exact time the vehicle passed the measurement point was determined using photoelectric sensors. The actual location of the measurement matrix is shown in Fig. 5.
The research was carried out in the Franowo tram depot in Poznan. The location of the measurement point within the depot is shown on the map in Fig. 6. The research was conducted for vehicles running on track no. 32 as it was the track on which the trams going down for maintenance passed. The object of the research was a low-floor Solaris Tramino S105p produced by Solaris Bus & Coach and operated by Miejskie Przedsiębiorstwo Komunikacyjne w Poznaniu Sp. z o. o. The structural diagram of the Solaris Tramino S105p tram is shown in Fig. 7.
Basic technical parameters of Solaris Tramino S105p tram are presented in Table 1.
It is a fully low-floor, articulated tram intended for one-way traffic. It is one of the basic vehicles used by the city operator. Thanks to that, the number of rolling stock was ensured at a level making it possible to conduct the experiment
A modular measuring apparatus was utilized to carry out the study. In the measurements, a condenser matrix microphone type B&K 4958 was used, which was also intended for measurements of non-stationary signals, i.e. those which were to be acquired during the experiment. They allowed registration in the frequency band of 20-20 000 Hz. A pair of BX15M-TDT photoelectric sensors was used to record the moment the trams passed the measuring station. To record and archive the signals, we used a PULSE 9727 system with a B&K 3560C data acquisition module enabling lossless, synchronous recording of signals in all channels in the band from 0 to 25.6 kHz (at a sampling rate of 65 536 Hz).
Control of the measurement apparatus and data recording were performed using a personal computer equipped with BK Connect 2018 software.

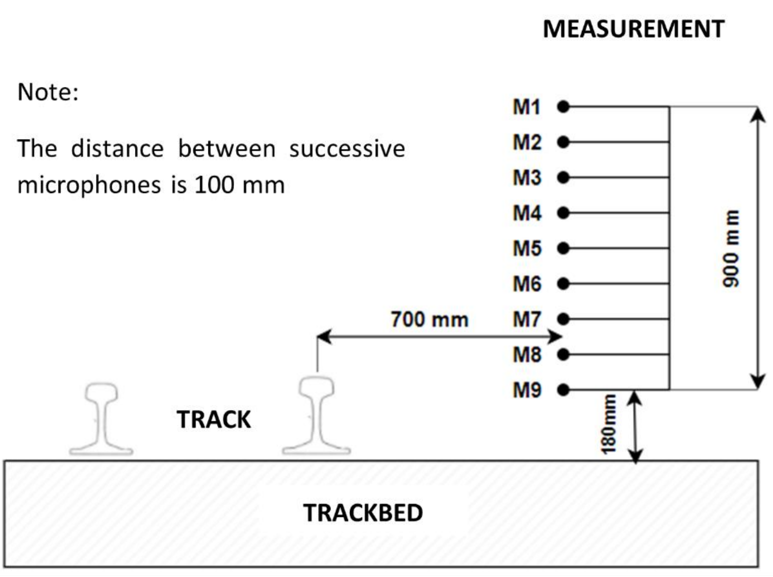

Fig. 4. Test stand scheme [own elaboration]

Fig. 5. Location of the measurement matrix [own elaboration]

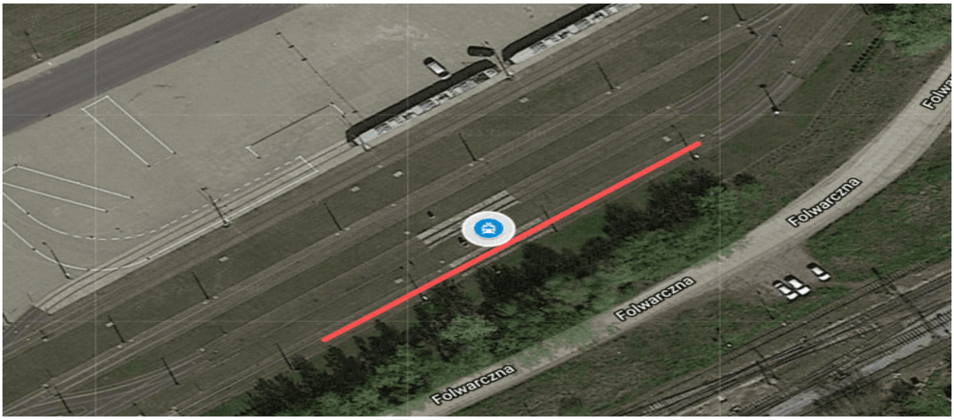

Fig. 6. Test site. Pictogram - measurement stand, red line - track no. 32, on which the tested trams were running [own elaboration based on ©Google Maps 2022]

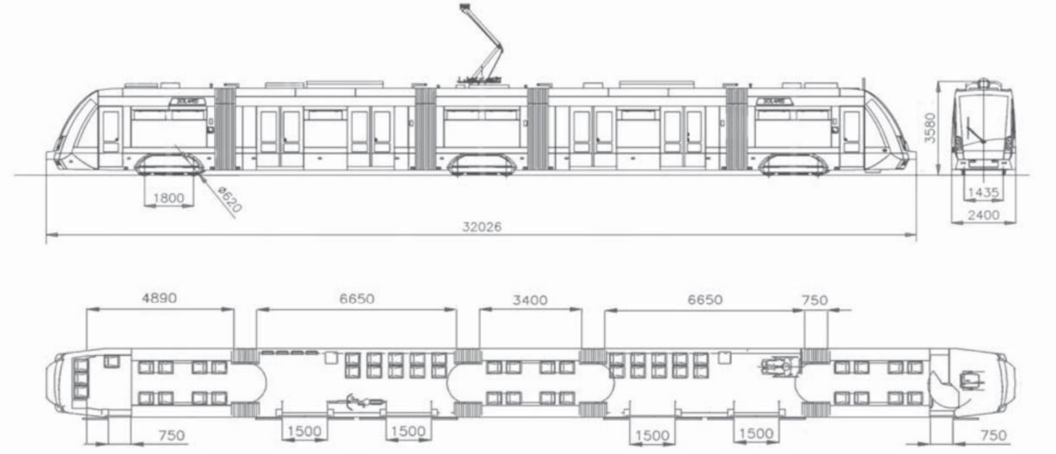

Fig. 7. Construction diagram of the Solaris Tramino tram S105p (Solaris Bus & Coach Sp. z. o. o., 2017)

Table 1. The selected technical parameters of the Solaris Tramino S105p

Total length	32 026 mm	Number of bogies	3
Width of car body	2 400 mm	Track width	1 435 mm
Internal width of car body	2 195 mm	Diameter of new wheels	620 mm
Height with pantograph folded	3 760 mm	Diameter of worn wheels	540 mm
Number of sections	5	Floor height above rail head	350 mm

5. Analysis and signal processing

The analysis of the obtained data was carried out with the use of the BK Connect program, which is a software dedicated to operating the measuring equipment of Brüel & Kjær. Based on the measurement cards prepared during the experiment, the measurements subject to further processing were selected. Tram passes that were accompanied by interference that could influence the final results, e.g. during the simultaneous passage of another vehicle on the adjacent track, or during a freight train passage at the nearby freight station Poznań Franowo, were rejected. The rolling stock list was then sent to the operator with a request to indicate whether any of the examined trams had a defect in the drive system, and if so, what kind it was.

Based on the data from the operator two pairs of trams were chosen. The trams in the pair travelled at identical speeds, one was operational and the other had damage in the transmission system. In both cases the damage was of similar nature and was located in the traction gear on the third bogie.

The analysis was conducted for the first pair. First, the possibility of using STFT to detect the damage was evaluated. Then the analogous step was performed for CWT. In the last step, the feasibility of using a combined CWT-Cepstrum method was analyzed.

The second pair was used to validate the combined method to verify if it is possible to repeat its successful use on other vehicles.

5.1. Preliminary analysis of signals in the time domain

First, a diagnostically useful signal was extracted from the measurements made. For this purpose, the simultaneous recording of the acoustic signal from the microphones and the voltage magnitude from the photoelectric sensor was used, which recorded the voltage of 5 V at the moment of circuit interruption caused by the passage of the tested vehicle. In this way, the acoustic signals obtained could be limited only to the moment of passing and thus determine the vehicle speed and the location of the gear and drive systems.

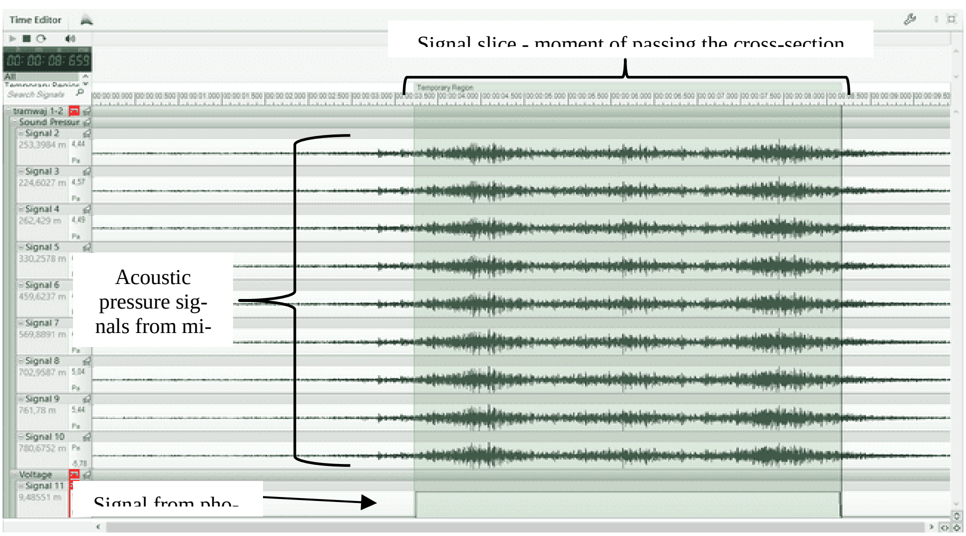

Fig. 8. Signal selection using measurements from a photocell

As a result of cooperation with the operator, two pairs of trams were selected for further analysis - the first pair with serial numbers 543 and 555, the second pair with serial numbers 533 and 556. Trams No. 533 and 543 were undamaged, while in the case of 555 and 556 damage was found in the traction gear of the third bogie in the form of broken teeth. The presented paper focuses only on the signal processing methods themselves, omitting the analysis of the location of measuring points. Therefore, the acoustic pressure recorded by the central microphone of matrix #5 located at a height of 580 mm from the upper limit of the substructure was selected for further study. The main part of the research is conducted in this paper on the pair 543-555. Its time course of the recorded sound pressure is shown in Fig. 9.

To evaluate the stationarity of the signals, we used the evaluation of the correlation of the signal with its successive shifted forms according to equation 2. The course of the autocorrelation as a function of shift is shown in Figure 10.

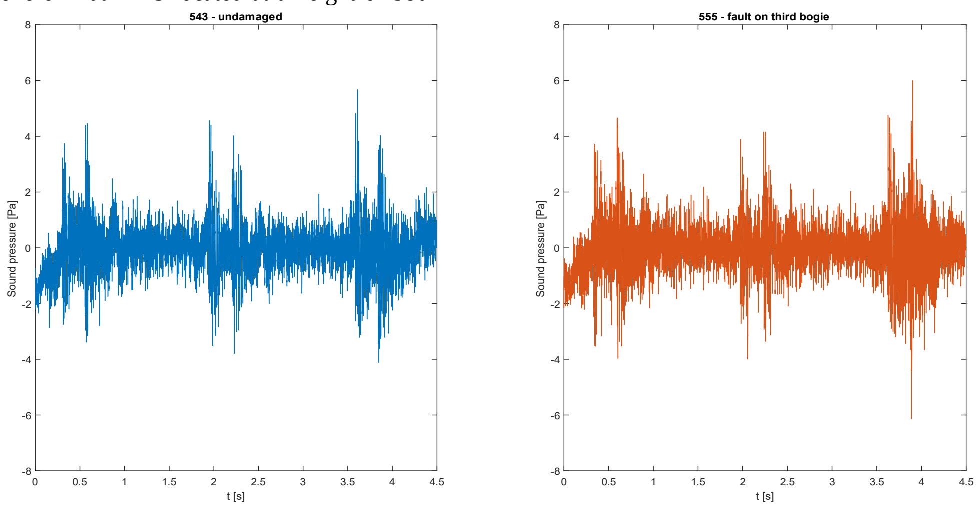

Fig. 9. Time course of sound pressure for 543 and 555 vehicle passes

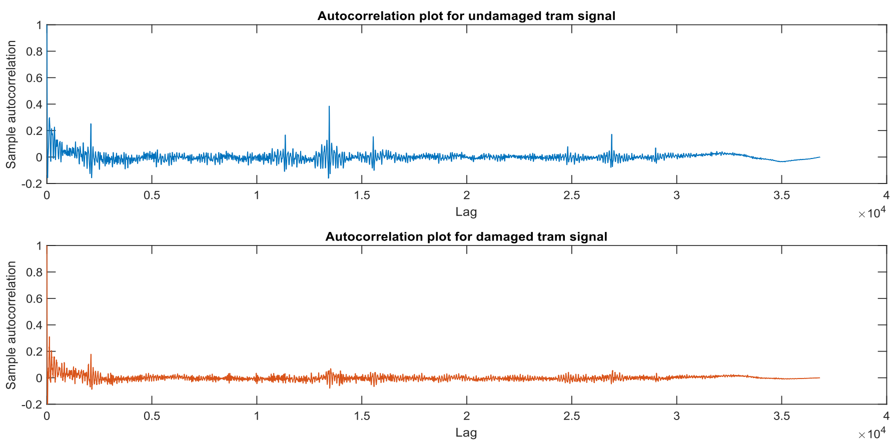

Fig. 10. Autocorrelation characteristics as a function of signal shift for vehicles 543 (undamaged) and 555 (damaged)

Analyzing the characteristics in Fig. 10, one finds a low correlation of the signal with respect to its shifted version, both for the efficient and damaged case. While for tram 543 a recurrent increase in autocorrelation can be observed for some shift values (lag for n~2 400, 13 500, 26 000) resulting from superposition in the signal of moments of passing the measuring station by the bogies of the tested vehicles, in the damaged case no periodicity in the level of correlation can be found. This allows us to conclude that in the analyzed case the autocorrelation depends on time, which means that the conditions of signal stationarity are not met and methods dedicated to non-stationary signals should be used.
Based on the length of the tested vehicles known from the diagram in Fig. 7 and the time of occurrence of 5 V voltage on the signal from the photocell, it was possible to estimate the vehicle speed according to equation 10.

$$V_t = \frac{L_t}{t} \tag{10}$$

where:
V_t – average speed of the tested vehicle [m/s]
Lt – length of tested vehicle [m]
t – obstacle detection time on photoelectric sensor [s]
The obtained speed is an average speed, as small accelerations or decelerations may have occurred while passing the measurement point.
In order to analyze the technical efficiency of the tested drive systems, the characteristic frequencies of their individual components had to be determined. On the basis of the known speed of the individual vehicles and the extreme values of the wheel diameter as given by the manufacturer, their rotational frequencies were determined in accordance with equation 11.

$$f_{rot_{wheel}} = \frac{V_t}{\pi \cdot d} \tag{11}$$

where:
V_t – average speed of tested vehicle [m/s]
d – wheel diameter [m]
The frequencies of the wheels are simultaneously represented by the frequencies of the shaft on which they are arranged.
The next stage of the drive testing was to determine the technical parameters and characteristic frequencies of the traction gear of the Solaris S105p tram. According to the technical documentation, it is a two-stage transmission consisting of five gears - two bevel gears and three straight gears arranged in three kinematic pairs. The number of teeth in each wheel was: $z_1 = 14$, $z_2 = 27$, $z_3 = 19$, $z_4 = 51$, $z_5 = 66$.
In order to determine the characteristic frequencies of the remaining shafts, the gear ratios should be calculated using equations 12-14.

$$i_{s1} = \frac{z_2}{z_1} \cdot \frac{z_4}{z_3} \cdot \frac{z_5}{z_4} \tag{12}$$

$$i_{s2} = \frac{z_4}{z_3} \cdot \frac{z_5}{z_4} \tag{13}$$

$$i_{s3} = \frac{z_5}{z_4} \tag{14}$$

where i_{sn} – ratio on n shaft.
Knowing the ratios of the individual shafts, their rotational speeds were determined according to equation 15.

$$f_{rot_{sn}} = i_{sn} \cdot f_{rot_{s4}} \tag{15}$$

where f_{rotsn} – rotational speed of n shaft.
Next, the meshing frequency of individual gears was determined in accordance with equations 16-17.

$$f_{z1} = f_{rot_{s1} \cdot z_1} = f_{z2} \tag{16}$$

$$f_{z3} = f_{rot_{s2} \cdot z_3} = f_{z4} = f_{z5} \tag{17}$$

where f_{zn}– gear meshing frequency n.
The results of the characteristic frequency calculations are shown in Table 2.

Table 2. Characteristic frequencies of kinematic pairs of transmissions in selected analyzed pairs of vehicles

Pair	**Speed [km/h]**	**Wheel meshing frequency 1-2 [Hz]**		**Wheel meshing frequency 3,4,5 [Hz]**	
		Unworn	**Worn**	**Unworn**	**Worn**
555(D)-543	23.7	317	364	223	256
556(D)-533	21.4	286	329	201	231

By analyzing Table 2, it can be concluded that the range of characteristic frequencies for the first pair is in the set <223 Hz; 364 Hz>, and for the second pair in the set <201 Hz; 328 Hz>. The determined characteristic frequencies were further used to interpret the time-frequency maps and the CWT-Cepstrum method for the individual tested vehicles.

5.2. Time-frequency analysis using STFT

The main stage of analysis of the recorded acoustic signal was its decomposition in the time-frequency domain. The aim of this action was primarily to locate in the studied characteristics of the sources of noise generated by individual elements of the three bogies. The STFT described by equation 8 in discrete form was used. In accordance with the Nyquist-Shannon theorem, the sampling frequency used allows for analyzing the signal in the frequency band of 1-25 kHz, while the range of microphones used was 1-20 kHz. Due to the determined characteristic frequencies, the frequency band was limited to 1.6 kHz. The next issue considered was the size of the window under study. The analysis was performed using a Hannig window and exponential spectrum averaging. The window size was 2 Hz in the frequency domain and 500 ms in the time domain with an averaging time of 166.7 ms. A comparison of the spectrograms for the case of an operable vehicle (543) and with a damaged traction transmission in the third bogie (555) is shown in Fig. 11.

The tram with rolling stock number 543 was moving at a speed similar to that of tram number 555, thus a comparative analysis of the acoustic signal in the range of characteristic frequencies can be carried out. In the signal of the third bogie of the vehicle 555 with a potential transmission failure, the appearance of additional harmonics with high amplitudes is visible, which are not present in the other bogies or in the third bogie of the tram 531. The appearance of such components indicates a malfunction in the transmission system (Nowakowski, 2020). An increased sound pressure level is also observed at 308 Hz (18 dB difference with respect to the undamaged one), which is within the characteristic frequency range. In addition, increased sound was observed at 640 Hz and 964 Hz (difference of 17 dB and 19 dB, respectively, relative to the intact).

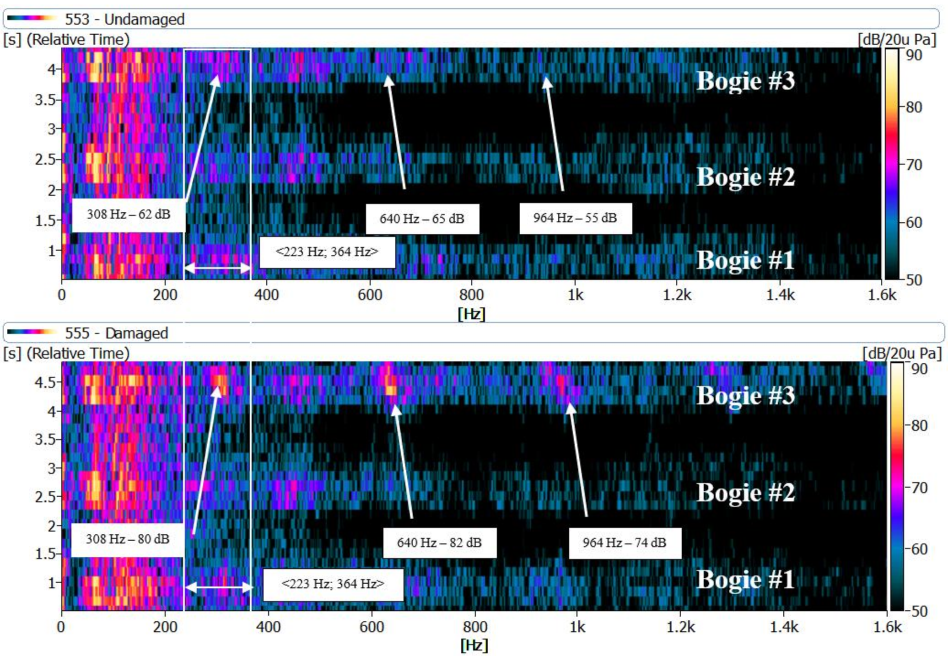

Fig. 11. STFT analysis of acoustic signal for undamaged vehicle 543 (top) and with damaged third bogie 555 (bottom) - sound level dB SPL

The above observations allow us to conclude that STFT can be helpful in terms of damage detection and localization. However, one should keep in mind the limitations associated with the fixed window resolution. Attempting to obtain more precise information in the frequency range will result in a loss of quality in terms of damage location information. More precise localization will result in a loss of quality in the frequency domain, harmonic bands may change. Therefore, this method should be treated as a qualitative aid in determining suspected damage.

5.3. Time-frequency analysis using CWT

Limitations in the use of the STFT have necessitated the development of alternative methods for processing non-stationary signals. One of them is the wavelet transform, which uses mother wavelets as the kernel of the transform. Their number to use is infinite, moreover they can be scaled and shifted which determines their high potential in time-frequency signal processing. This is at the same time a disadvantage, changing the wavelet used or altering its attributes can produce different results, making subsequent interpretation difficult. The different way of forming windows in WV should also be taken into account. Unlike the fixed-dimensional STFT windows, with the wavelet transform the windows are automatically scaled as shorter for lower frequencies and longer for higher frequencies. This allows the signal to be interpreted from a different perspective, time-scale (scalogram) instead of time-frequency (spectrogram). Figure 12 shows a comparative analysis of the scalograms for an operable vehicle (543) and a vehicle with a failed traction transmission in the third bogie (555). A db6 wavelet was used at a sampling rate of 8192 Hz.

The time-scale characteristic presented in Fig. 12 is visibly different from the time-frequency characteristic obtained with the use of STFT. Another method of window formation and the mother wavelet used revealed in the instantaneous signal lasting 0.1 seconds significant increases in the sound level in a wide range of scales. They result from registering in the acoustic signal the moment of the wheel sets' overrun on the rail joints. The scale parameter does not simply translate into the frequency of the signal. It is not possible, however, to simply analyze the scalogram in the frequency range of the characteristic gears. There is, however, an approximate relationship between scale and frequency using the center frequency of a given mother wavelet. Due to the approximation, the obtained value is called pseudofrequency and is described by equation 18 (Prieto-Guerrero & Espinosa-Paredes, 2019):

$$F_a = \frac{F_c}{a \cdot \Delta} \tag{18}$$

where:
Fa – pseudofrequency corresponding to the adopted scale [Hz]
Fc – center frequency of the mother wavelet [Hz]
a – scale parameter
Δ – sampling period

Equation 18 shows that the relationship between scales and frequency is inversely proportional i.e. as the scale increases, the corresponding pseudofrequency decreases. After conversion, the range of scales analyzed was limited to the set <17;26>. The transformation into pseudofrequencies corresponding to particular scales is presented in Table 3.

The range of scales shown in Table 3 does not directly coincide with the calculated characteristic frequencies shown in Table 2. This is because attempting to expand the set will cause the characteristic frequencies to go beyond the set limits.

Figure 12 shows an increase in sound level for the range of scales from 10 to 21 for the third bogie of the damaged vehicle. This increase does not occur in the functional vehicle. The set of scales <10;21> overlaps partially with the set <17;26> which means that an increase in the sound level due to transmission damage is observed in the characteristic frequency range. For scale 17, the sound level is about 105 dB SPL with the damaged case compared to 91 dB SPL with the undamaged case.

Based on the above observations, it can be concluded that CWT can be helpful in terms of damage detection and localization. However, it is not a perfect method. The difficulty is that there is no direct relationship between the scale domain and the frequency domain. Only an approximated transformation of the scales to the corresponding pseudofrequencies associated with the center frequencies of the applied mother wavelets is possible. Thus, this method should be treated as a qualitative one indicating the possibility of damage.

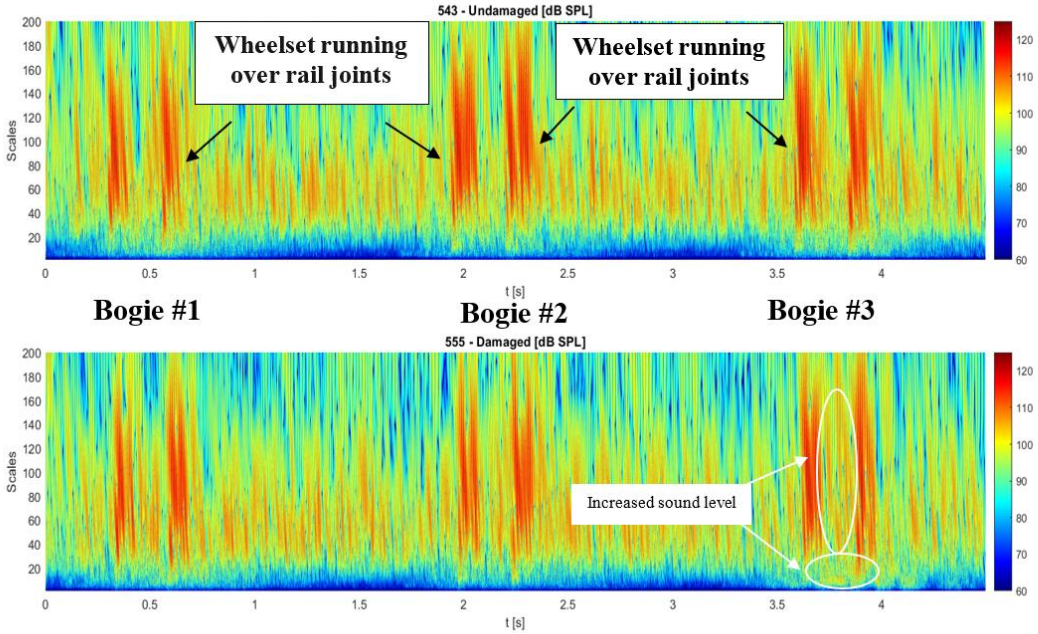

Fig. 12. CWT analysis of acoustic signal for vehicle 543 (top) and 555 (bottom) - db6 wavelet, scale range 1:200 - sound level dB SPL

Table 3. Summary of scales and corresponding pseudofrequencies for db6 wavelet and sampling rate

Scale	Pseudofrequency (Hz)	Scale	Pseudofrequency (Hz)
17	350	22	271
18	331	23	259
19	314	24	248
20	298	25	238
21	284	26	229

5.4. Application of the combined CWT-Cepstrum method

The limitations and difficulties associated with the correct interpretation of time-frequency and time-scale representations make it necessary to develop more accurate methods allowing for more precise signal analysis. The solution proposed by the authors is to use the cepstrum as a complement to the signal processing using the continuous wavelet transform due to the demonstrated effectiveness of the cepstrum in diagnosing drive systems and their components. The CWT would serve in such a solution as a pre-filter of the tested signal. The advantage over traditional frequency filters is the possibility of signal decomposition not only in terms of scales but also in terms of mother wavelet selection.

In the investigated pair of trams, after preliminary analysis, the use of wavelet coefficients for scale 70 (with preservation of previous CWT parameters i.e. mother wavelet db6 and analysis range of 1:200 scales) was found to be the most appropriate. An attempt to use scales from the range of pseudofrequencies corresponding to the set of characteristic frequencies (from 17 to 26) resulted in the fundamental frequency of the obtained cepstrum going beyond this set. The fragment corresponding to the sound pressure measurement for the third bogie was then cut from such a signal (Fig. 13).

Interpretation of the signal as shown in Fig. 13 is difficult in the context of determining the presence of damage to the drive components. This is due to both noise and large amplitude increases associated with the overrun on the track joint. This justifies further signal processing using a cepstrum, which is characterized by its sensitivity to vibroacoustic processes caused by the kinematic interaction of the transmission components. The cepstrum indicates to us the existence of periodic components in the signal spectrum, e.g. harmonics or sidebands equally spaced apart. Fig. 14 shows a comparison of the undamaged and damaged case processed using three forms of cepstrum.

A signal processed using a cepstrum represented in the quefrency domain, whose measure is time. However, this measure is not the same as the analog in the time domain. The transformation from the quefrency domain to the frequency domain is performed using the relationship between the period and the frequency (equation 19).

$$f_h = \frac{1}{T} \tag{19}$$

where:

f_h – frequency of the analysed component [Hz]

T – quefrency of the analysed component [s]

Analyzing the individual cepstra, it can be concluded that in the case studied, the real and power forms have the greatest diagnostic value (where it can be seen that one form is a rescaled form of the other). The composite form (presented on the characteristic in the form of an absolute quantity) containing information about the phase shift of the signal due to noise makes the analysis difficult in the range of characteristic frequencies of the transmission. In the real and power cepstrum of the damaged case the periodic frequency components are revealed for quefrency 4.418 ms, 7.952 ms and 10.77 ms, which corresponds to 226.35 Hz, 125.75 Hz, 92.85 Hz respectively. In the undamaged case, only the former appears. It is the fundamental frequency for the signal and it is within the examined range of characteristic frequencies of the diagnosed transmission. There is visible increase of its amplitude in case of damage.

5.5. Validation of the CWT-Cepstrum combined method on an independent case

In order to validate the method, a second pair of trams was analysed under similar conditions. One of the vehicles was fully operational, while in the other one a transmission failure was detected in the form of broken teeth in the gears. A The real and power cepstrum again revealed a fundamental frequency of 4.418 ms which corresponds to 226.5 Hz and is in the characteristic frequency range. For the damaged transmission, the amplitude of the fundamental component is visibly higher than for the efficient transmission. Additional periodic components of 7.714 ms corresponding to 129.63 Hz, 10.89 ms corresponding to 91.83 Hz and 18.82 corresponding to 53.13 Hz are also revealed. Out of which the last two components are suppressed in the power cepstrum. The results of the analysis confirm that the method can be used effectively for more than a case making it a potentially effective diagnostic tool.

In the last step, it was undertaken to verify the method for the existence of an error that would always generate an increased amplitude of the fundamental frequency and additional periodic components in one of the cases (so-called artifacts) which would cause false detection of the damage. Thus, a third pair consisting only of the efficient cases 533-543 was constructed.The results are shown in Fig. 16.gain the filtering was performed using CWT - db6 wavelet and scale 70. The results are presented in Fig. 15.

The real and power cepstrum again revealed a fundamental frequency of 4.418 ms which corresponds to 226.5 Hz and is in the characteristic frequency range. For the damaged transmission, the amplitude of the fundamental component is visibly higher than for the efficient transmission. Additional periodic components of 7.714 ms corresponding to 129.63 Hz, 10.89 ms corresponding to 91.83 Hz and 18.82 corresponding to 53.13 Hz are also revealed. Out of which the last two components are suppressed in the power cepstrum. The results of the analysis confirm that the method can be used effectively for more than a case making it a potentially effective diagnostic tool.

In the last step, it was undertaken to verify the method for the existence of an error that would always generate an increased amplitude of the fundamental frequency and additional periodic components in one of the cases (so-called artifacts) which would cause false detection of the damage. Thus, a third pair consisting only of the efficient cases 533-543 was constructed.The results are shown in Fig. 16.

As expected, the results do not deviate from each other, with differences in amplitude being minimal. In the case of the real cepstrum and power, it is also not possible to conclude that the cepstrum signal for one vehicle contains components absent in the cepstrum signal of the other. In the case of the combined cepstrum, the signal analogously to the previous cases is difficult to analyze. The presented results allow to conclude that the proposed method does not generate artifacts that could falsely indicate a non-existing damage.

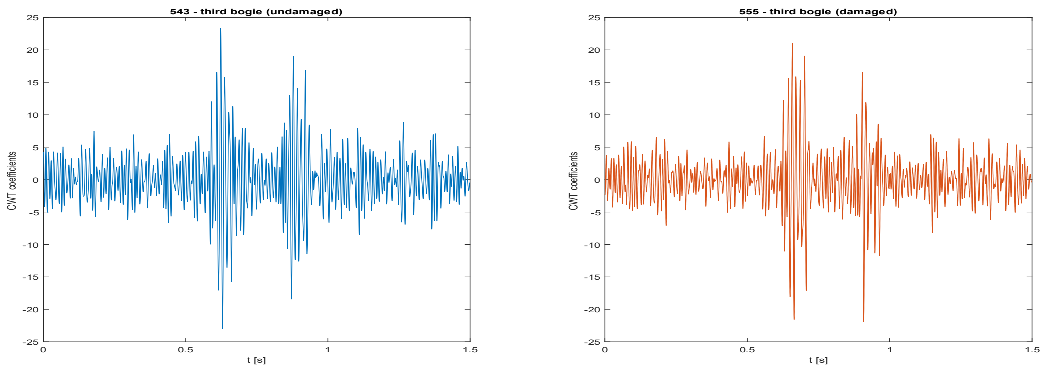

Fig. 13. Time course of wavelet coefficients for mother wavelet db6 and scale 70 - fragment for the third bogie

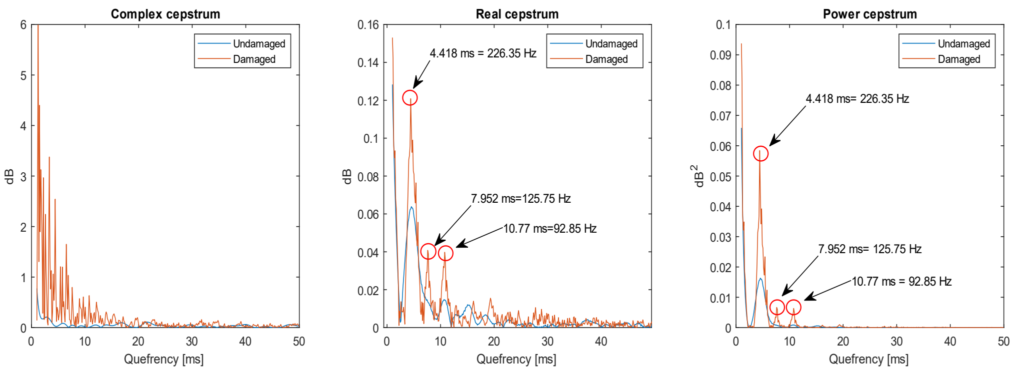

Fig. 14. Different forms of cepstrum from CWT-filtered signal for 543(undamaged)-555(damaged) pair)

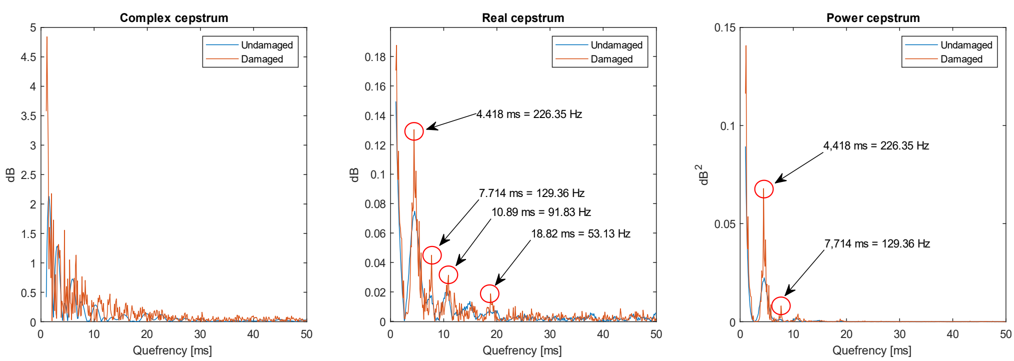

Fig. 15. Different cepstrum forms from the CWT-filtered signal for the 533(undamaged)-556(damaged) pair)

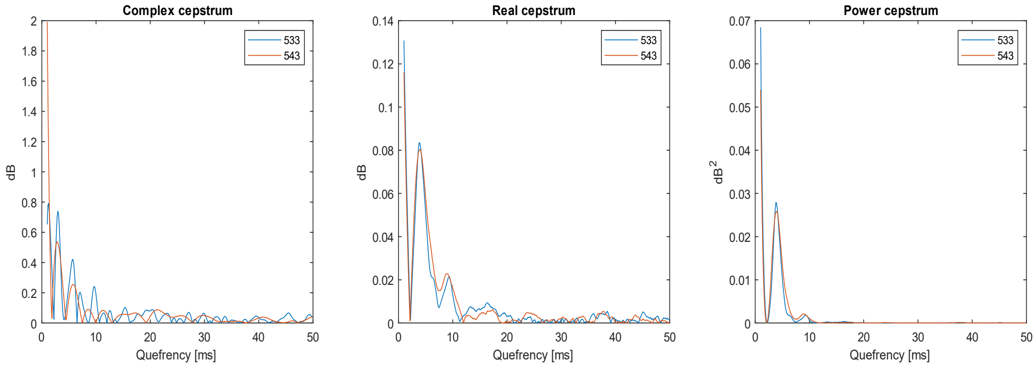

Fig. 16. Different forms of cepstrum from CWT-filtered signal for pair 533-543 (both undamaged)

5.6. Summary of analysis

Analyzing the results obtained with the combined method of CWT and cepstrum, it can be concluded that pre-filtering the signals with wavelet transform to eliminate the problem of non-stationarity of signal in time, and then using the properties of cepstral analysis to identify the occurrence of damage symptoms in the analyzed signal can be an effective method for vibroacoustic diagnostics of railway vehicle drive systems. The resulting defects cause an increase in the fundamental frequency amplitude, as well as additional periodic components in the cepstrum. However, one should keep in mind the sensitivity of the method to the assumed boundary conditions of the analysis. A crucial aspect of filtering a signal using CWT is the selection of an appropriate mother wavelet. Even if all other conditions are kept unchanged, its change can cause extremely different results. It is also important to choose an appropriate scale, which is inversely related to increasing frequency. The scale should be chosen so that the fundamental frequency after processing is within the range of characteristic frequencies of the tested transmission. The presented method due to easy acquisition of the diagnostic parameter (sound recording even from a single microphone) has an application potential. A further step could be to perform an active experiment and record a statistically significant number of vehicle passes with different transmission conditions. From this, it would be possible to determine the amplitude thresholds of the fundamental frequency corresponding to the characteristic frequency after CWT-cepstrum processing and thus automate the identification of defects based on the measurement of sound pressure only.

6. Conclusions

Based on the calculations performed and the time-frequency and time-scale representations obtained, we conclude that they are useful for damage detection in the case described. In the case of both transforms, damage to the transmission translated into visible changes in both spectrograms and scalograms relative to the undamaged vehicle. Thanks to simultaneous analysis in the time and frequency/scale domains, it was possible to precisely locate in which bogie the defect occurred and to indicate what effect it had on the frequency components of the signal. Thanks to the knowledge of characteristic frequencies of the traction transmission, it was possible to associate the increase of acoustic pressure level for some frequency components with the occurrence of a defect in this particular transmission.

However, these methods have some limitations in application. The effectiveness of STFT is limited by the fixed window resolution problem. CWT despite its better scaling properties than STFT is limited by the physical sense of the scaling parameter, which cannot be accurately converted to frequency, and is also sensitive to the selection of the mother wavelet. The presented new CWT-Cepstrum method used the wavelet transform as a filter for the signal under study. The wavelet coefficients for the selected value of the scale parameter were constrained to the sound pressure recorded in the test for the third bogie and then transformed with three forms of cepstrum: complex, real and power. In terms of drive system diagnostics, the latter two forms of cepstrum were most useful. Damage in the form of gear tooth breakage caused a significant increase in amplitude for the periodic frequency component of 226.35 Hz, as well as the generation of additional periodic components at 125.75 Hz and 92.85 Hz. It is also possible to successfully replicate the use of the method for other tram test pairs, the method does not generate false positives for test pairs composed of operable vehicles.

The presented results allow concluding that the proposed method can be effectively used for diagnostics of drive components, i.e. traction transmission in the case studied. Moreover, due to easy acquisition of the diagnostic parameter (sound recording even from a single microphone) it has an application potential.

Acknowledgements

The presented results have been co-financed from the subsidies appropriated by the Ministry of Education and Science - 0416/SBAD/0003 and 0416/SBAD/0004.

References

[1] Jaworek, K., Kownacki, C., Pauk, J. (2001). Wavelet transform - a modern tool in measured signal analysis (in Polish). *Scientific Journals of the Białystok University of Technology. Construction and Operation of Machines*, 199–212.

[2] Jiang, F., Ding, K., He, G., Du, C. (2021). Sparse dictionary design based on edited cepstrum and its application in rolling bearing fault diagnosis. *Journal of Sound and Vibration*, *490*, 115704. https://doi.org/10.1016/j.jsv.2020.115704.

[3] Johansson, A., Andersson, C. (2005). Out-of-round railway wheels—a study of wheel polygonalization through simulation of three-dimensional wheel–rail interaction and wear. *Vehicle System Dynamics*, *43*(8), 539–559. https://doi.org/10.1080/00423110500184649.

[4] Katunin, A., Dragan, K., Dziendzikowski, M. (2015). Damage identification in aircraft composite structures: A case study using various non-destructive testing techniques. *Composite Structures*, *127*, 1–9. https://doi.org/10.1016/j.compstruct.2015.02.080.

[5] Kehtarnavaz, N. (2008). *Digital Signal Processing System Design*. Elsevier. https://doi.org/10.1016/B978-0-12-374490-6.X0001-3.

[6] Kim, Y., Ha, J. M., Na, K., Park, J., Youn, B. D. (2021). Cepstrum-assisted empirical wavelet transform (CEWT)-based improved demodulation analysis for fault diagnostics of planetary gearboxes. *Measurement: Journal of the International Measurement Confederation*, *183*(July), 109796. https://doi.org/10.1016/j.measurement.2021.109796.

[7] Komorski, P., Nowakowski, T., Szymanski, G. M., Tomaszewski, F. (2018). Application of Time-Frequency Analysis of Acoustic Signal to Detecting Flat Places on the Rolling Surface of a Tram Wheel. In *Springer Proceedings in Mathematics and Statistics* (Vol. 249, pp. 205–215). Springer International Publishing. https://doi.org/10.1007/978-3-319-96601-4_19.

[8] Li, W., Cao, Y., Li, L., Hou, S. (2022). An Orthogonal Wavelet Transform-Based K-Nearest Neighbor Algorithm to Detect Faults in Bearings. *Shock and Vibration*, *2022*, 1–13. https://doi.org/10.1155/2022/5242106.

[9] Liang, B., Iwnicki, S., Feng, G., Ball, A., Tran, V. T., Cattley, R. (2013). Railway wheel flat and rail surface defect detection by time-frequency analysis. *Chemical Engineering Transactions*, *33*(January), 745–750. https://doi.org/10.3303/CET1333125.

[10] Liu, D., Cheng, W., Wen, W. (2020). Rolling bearing fault diagnosis via STFT and improved instantaneous frequency estimation method. *Procedia Manufacturing*, *49*, 166–172. https://doi.org/10.1016/j.promfg.2020.07.014.

[11] Lopez-Ramirez, M., Romero-Troncoso, R. J., Morinigo-Sotelo, D., Duque-Perez, O., Ledesma-Carrillo, L. M., Camarena-Martinez, D., Garcia-Perez, A. (2016). Detection and diagnosis of lubrication and faults in bearing on induction motors through STFT. *2016 International Conference on Electronics, Communications and Computers (CONIELECOMP)*, 13–18. https://doi.org/10.1109/CONIELECOMP.2016.7438545.

[12] Lu, R., Shahriar, M. R., Borghesani, P., Randall, R. B., Peng, Z. (2022). Removal of transfer function effects from transmission error measurements using cepstrum-based operational modal analysis. *Mechanical Systems and Signal*

Processing, *165*, 108324. https://doi.org/10.1016/j.ymssp.2021.108324.

[13] Lyon, R. H., Ordubadi, A. (1982). Use of Cepstra in Acoustical Signal Analysis. *Journal of Mechanical Design*, *104*(2), 303–306. https://doi.org/10.1115/1.3256340.

[14] Majeed, R., Haddar, M., Chaari, F., Haddar, M. (2023). *A Wavelet-Based Statistical Control Chart Approach for Monitoring and Detection of Spur Gear System Faults* (pp. 140–152). https://doi.org/10.1007/978-3-031-34190-8_17.

[15] Mandic, D. P., Rehman, N. ur, Wu, Z., Huang, N. E. (2013). Empirical Mode Decomposition-Based Time-Frequency Analysis of Multivariate Signals: The Power of Adaptive Data Analysis. *IEEE Signal Processing Magazine*, *30*(6), 74–86. https://doi.org/10.1109/MSP.2013.2267931.

[16] Milewicz, J., Mokrzan, D., Szymański, G. (2021). The assessment of the technical condition of SO-3 engine turbine blades using an impulse test. *Combustion Engines*, *184*(1), 24–29. https://doi.org/10.19206/CE-133872.

[17] Milewicz, J., Mokrzan, D., Szymański, G. M. (2023). Environmental Impact Evaluation as a Key Element in Ensuring Sustainable Development of Rail Transport. *Sustainability*, *15*(18), 13754. https://doi.org/10.3390/su151813754.

[18] Mokrzan, D., Milewicz, J., Szymański, G., Szrama, S. (2021). Vibroacoustic analysis in the assessment of the technical condition of the aircraft airframe composite elements. *Diagnostyka*, *22*(2), 11–20. https://doi.org/10.29354/diag/135098.

[19] Mokrzan, D., Szymański, G. (2021). Time-frequency methods of non-stationary vibroacoustic diagnostic signals processing. *Rail Vehicles*, *3*, 44–57. https://doi.org/10.53502/RAIL-143047.

[20] Newland, D. E. (1997, September 14). Practical Signal Analysis: Do Wavelets Make Any Difference? *Volume 1A: 16th Biennial Conference on Mechanical Vibration and Noise*. https://doi.org/10.1115/DETC97/VIB-4135.

[21] Nowakowski, T. (2020). *Development of a method for assessing tram vibroacoustic activity based on trackside measurements. Doctoral thesis (in Polish)*. Poznan University of Technology.

[22] Nowakowski, T., Komorski, P., Szymański, G. M., Tomaszewski, F. (2019). Wheel-flat detection on trams using envelope analysis with Hilbert transform. *Latin American Journal of Solids and Structures*, *16*(1). https://doi.org/10.1590/1679-78255010.

[23] Ortiz, J., Betancur, G. R., Gómez, J., Castañeda, L. F., Zając, G., Gutiérrez-Carvajal, R. (2018). Detection of structural damage and estimation of reliability using a multidimensional monitoring approach. *Proceedings of the Institution of Mechanical Engineers, Part F: Journal of Rail and Rapid Transit*, *232*(4), 1021–1032. https://doi.org/10.1177/0954409717707122.

[24] Ouamara, D., Boukhnifer, M., Chaibet, A., Maidi, A. (2023). Diagnosis of ITSC fault in the electrical vehicle powertrain system through signal processing analysis. *Diagnostyka*, *24*(1), 1–10. https://doi.org/10.29354/diag/161309.

[25] Park, K. Il. (2018). *Fundamentals of Probability and Stochastic Processes with Applications to Communications*. Springer.

[26] Prieto-Guerrero, A., Espinosa-Paredes, G. (2019). Linear signal processing methods and decay ratio estimation. In *Linear and Non-Linear Stability Analysis in Boiling Water Reactors* (pp. 269–314). Elsevier. https://doi.org/10.1016/B978-0-08-102445-4.00006-0.

[27] Randall, R. B. (1975). Gearbox fault diagnosis using cepstrum analysis. *World Congr on the Theory of Mach and Mech, 4th*, 169–174.

[28] Randall, R. B. (2011). Vibration-based Condition Monitoring. In *Vibration-Based Condition Monitoring: Industrial, Aerospace and Automotive Applications*. Wiley. https://doi.org/10.1002/9780470977668.

[29] Randall, R. B. (2017). A history of cepstrum analysis and its application to mechanical problems. *Mechanical Systems and Signal Processing*, *97*, 3–19. https://doi.org/10.1016/j.ymssp.2016.12.026.

[30] Rhif, M., Ben Abbes, A., Farah, I., Martínez, B., Sang, Y. (2019). Wavelet Transform Application for/in Non-Stationary Time-Series Analysis: A Review. *Applied Sciences*, *9*(7), 1345. https://doi.org/10.3390/app9071345.

[31] Saini, K., Dhami, S. S., Vanraj. (2022). Predictive Monitoring of Incipient Faults in Rotating Machinery: A Systematic Review from Data

Acquisition to Artificial Intelligence. *Archives of Computational Methods in Engineering*, *29*(6), 4005–4026. https://doi.org/10.1007/s11831-022-09727-6.

[32] Sapy, G. (1975). Application of Numerical Treatment of Signals for Vibration Diagnostic of Breakdowns: Detection of Fractures of Moving Blades. *Automatisme*, *20*(10), 392–399.

[33] Shim, J., Kim, G., Cho, B., Koo, J. (2021). Application of Vibration Signal Processing Methods to Detect and Diagnose Wheel Flats in Railway Vehicles. *Applied Sciences*, *11*(5), 2151. https://doi.org/10.3390/app11052151.

[34] Solaris Bus Coach Sp. z. o. o. (2017). *Tramino's product catologue*.

[35] Staśkiewicz, T., Firlik, B. (2018). Out-of-round tram wheels – current state and measurements. *Archives of Transport*, *45*(1), 83–93. https://doi.org/10.5604/01.3001.0012.0946.

[36] Szymański, G. M., Misztal, A., Misztal, W. (2017). Application of short time-frequency analysis to determine the extortion frequency of a jet aircraft engine on a test bench. *Autobusy: Technika, Eksploatacja, Systemy Transportowe*, *18*(12), 1328–1332.

[37] Tang, C., Zhao, Z., Shao, Y. Bin, Long, H., Du, Q. (2020). An Adaptive Time Delay Estimation Method for Broadcast Audio Based on Power Cepstrum. *Procedia Computer Science*, *166*, 258–263. https://doi.org/10.1016/j.procs.2020.02.103.

[38] Tatara, T., Kożuch, B. (2016). Propagation analysis of ground vibration caused by running trains with the use of FFT and STFT (in Polish). *Research and Technical Papers of Polish Association for Transportation Engineers in Cracow. Series: Proceedings*, *109*(2), 177–189.

[39] Wu, J. Da, Chen, J. C. (2006). Continuous wavelet transform technique for fault signal diagnosis of internal combustion engines. *NDT and E International*, *39*(4), 304–311. https://doi.org/10.1016/j.ndteint.2005.09.002.

[40] Yu, M., Chen, W., Cui, J., Wang, J. (2022). Identifying rotor-stator rubbing positions based on intrinsic time scale decomposition-hjorth-cepstrum. *Journal of Vibration and Control*, 107754632110501. https://doi.org/10.1177/10775463211050172.

[41] Zhao, H., Liu, J., Chen, H., Chen, J., Li, Y., Xu, J., Deng, W. (2023). Intelligent Diagnosis Using Continuous Wavelet Transform and Gauss Convolutional Deep Belief Network. *IEEE Transactions on Reliability*, *72*(2), 692–702. https://doi.org/10.1109/TR.2022.3180273.

[42] Zhu, Q., Wang, Y., Shen, G. (2012). Research and Comparison of Time-frequency Techniques for Nonstationary Signals. *Journal of Computers*, *7*(4), 954–958. https://doi.org/10.4304/jcp.7.4.954-958.